Computational Analysis of Speed Accuracy Tradeoff

Marcin Penconek (m.penconek2@uw.edu.pl)
University of Warsaw

Research Article

Keywords:

Posted Date: March 9th, 2022

DOI: https://doi.org/10.21203/rs.3.rs-1415280/v1

Computational Analysis of Speed Accuracy Tradeoff

Marcin Penconek

Quantitative Psychology & Economics, University of Warsaw

Email address: m.penconek2@uw.edu.pl

Abstract

Speed-accuracy tradeoff (SAT) is a well-documented phenomenon in the decision-making of humans and animals, but its underlying neuronal mechanism remains unclear. While modeling approaches conceptualize SAT through the threshold-tuning hypothesis as adjustments to the decision threshold, the leading neurophysiological perspective is the gain modulation hypothesis which postulates that the SAT mechanism is implemented through the baseline firing rate and the speed of evidence integration. In this paper, I investigate alternative computational mechanisms of SAT and show that while the threshold-tuning hypothesis is qualitatively consistent with behavioral data, the gain modulation hypothesis is inconsistent with the data. In order to reconcile the threshold-tuning hypothesis with the neurophysiological observations, I consider the interference of alpha oscillations with the decision process and show that the desynchronization of alpha oscillations results in an increase of the baseline firing rate and the speed of evidence integration. While alpha oscillations increase the discriminatory power of the decision system, they slow down the decision process. This suggests that alpha oscillations interact with the SAT mechanism and this interaction provides an alternative explanation of why the increase of the baseline firing rate and the speed of evidence integration is observed during the speed condition.

1. Introduction

Despite decades of research on speed-accuracy tradeoff (SAT), the underlying neuronal mechanism behind its implementation in the brain remains unclear. The speed-accuracy tradeoff is the ability to adjust response time to either responding slowly with high accuracy or fast with a high error rate (Chittka, Skorupski, & Raine, 2009). The phenomenon was studied in humans (Woodworth, 1899; Garret, 1922; Wickelgren, 1977) and was also observed in other species, including primates, rodents, and insects.

The last two decades of neurophysiological research revealed the brain mechanism of decision making and showed that forming categorical decisions follows an integration to the bound process (Newsome, Britten and Movshon, 1989; Britten et al, 1992; Shadlen and Newsome, 2001; Riotman and Shadlen, 2002; Schall, 2001; Gold and Shadlen, 2002; Kable and Glimcher, 2009). The bounded integration framework was previously envisioned in system-level computational models such as the drift diffusion model (DDM; Ratcliff, 1978; Luce, 1986). In these models, SAT is conceptualized under the selective influence assumption through the threshold-tuning hypothesis postulating that the speed-accuracy tradeoff is a result of adjusting the decision threshold (Bogacz et al., 2006; Bogacz et al., 2010): if speed is a priority, the decision threshold is decreased, and a decision is made faster based on integrating less information, while if accuracy is a priority, the decision threshold is increased, leading to more information being accumulated at the expense of response time. It is assumed that changes in threshold levels imply changes in firing rates at which the process terminates. Thus, it is expected that the firing rate threshold at which the decision is made vary between conditions: is lower for speed priority and higher with emphasis on accuracy. However, experimental evidence does not confirm this expectation. On the contrary, dot motion discrimination experiments show that the recorded threshold firing rates of neurons integrating evidence in favor of the choice are consistent between trials and independent from the condition. This observation challenges the threshold-tuning hypothesis as possible implementation of SAT in the brain.

Several alternative hypotheses of the computational mechanism of speed-accuracy tradeoff have been considered (Standage et al., 2014). Neurophysiological studies suggest that both the baseline firing rates and the ramping rates of neuronal activity in the regions of the brain implicated for decision-making are higher in tasks emphasizing speed (van Veen et al., 2008; Ivanoff et al., 2008; Forstmann et al., 2008; Hanks et al., 2014; Heitz and Shall, 2012). These results suggest that SAT is controlled through the baseline firing rate, which affects the speed of integration. A mechanism behind such modulation was postulated by analyzing SAT with the biophysically realistic decision-making model based on the recurrent attractor network with leaky integrate-and-fire neurons (Wang, 2002; Wong and Wang, 2006). The mechanism involves non-selective excitatory and inhibitory inputs to the network performing evidence integration tasks (Lo and Wang, 2006; Furman and Wang, 2008; Standage et al., 2013, Lo, Wang and Wang, 2015).

However, the computational analysis supporting the gain modulation hypothesis is inconsistent with behavioral experiments. In experiments when accuracy is the priority, the average reaction time (RT) on erroneous decisions is longer than the reaction time on correct decisions. However, under the speed condition, RTs ending with errors are shorter than RTs ending with correct decisions (Smith and Ratcliff, 2004). Wang's model with an attractor network produces shorter mean decision times on erroneous than correct trials (Wong and Wang, 2006; Standage et al., 2011). This effect is inconsistent with the observed effects in the "speed" condition.

Furthermore, other neuronal mechanisms occurring before and during the decision process affect decision-making speed and accuracy. Presentation of a stimulus leads to the desynchronization of alpha oscillations (event-related desynchronization) followed by the increase of alpha power after task execution (Klimesch et al., 2006). The large referential value of alpha power during the anticipation period is positively correlated with performance (Vogt et al., 1998; Klimesch et al., 2000; Doppelmeyr et al., 2002) and is negatively correlated with decision time (Paluch et al, 2021). All these results suggest that alpha oscillations might interfere with SAT effects.

In this paper, I investigate alternative computational mechanisms of implementing SAT and show that the threshold-tuning hypothesis is qualitatively consistent with experimental data, while the gain modulation hypothesis (Standage et al, 2014) is inconsistent with experimental data. The argument showing the inconsistency of the gain modulation hypothesis with the experimental data is (at least partially) general and not model-specific. I also show that alpha oscillations that interfere with the decision process can explain the apparent inconsistency of the threshold-tuning hypothesis with neurophysiological observations.

The alternative computational mechanisms of implementing SAT are modelled based on experimental data of Rafiei and Rahnev (2021). The experiment uncovered non-linear relationships which can shed light on how SAT is implemented in the brain when the analysis is performed with a decision-making model based on the recurrent attractor network.

Rafiei and Rahnev (2021) behavioral experiment was conducted on human subjects and involved manipulation of speed-accuracy tradeoff by linking the level of incentives to response latency. The task was to identify the direction of the Gabor patch presented to subjects at the angle +45 or -45 degrees. The difficulty was controlled by the contrast of the patch. Five SAT levels and five levels of task difficulty were considered. The authors analyzed the impact of SAT condition on the difference in reaction time (RT) between erroneous and correct decisions, the ratio of standard deviation and mean RT, and the skewness of RT distributions. The experiment discovered a robust U-shape relationship between SAT levels and the difference in reaction time (RT) between erroneous and correct trials. With the emphasis on accuracy, reaction times on erroneous decisions were longer than correct ones (except the lowest contrast). The difference was in the range of 50 to 100ms, depending on the contrast level. I will refer to this pattern of RTs as the positive RT difference. When speed became a priority, RT before erroneous responses became shorter than RT preceding correct decisions (except the lowest contrast). The difference was in the range of -20 to -60ms. I will refer to this pattern of RTs as the negative RT difference. The above results are consistent with previous observations in behavioral studies on human subjects. Under the strongest emphasis on speed, the difference between RTs approached zero, i.e.,

the mean RT for erroneous decisions and the mean RT for correct decisions became roughly equal. The described effects produce the U-shape relationship between the difference on RTs for erroneous and correct trials and the SAT conditions. The results are intuitively correct as with the strongest emphasis on speed, the decisions are almost random, and no difference in RT between correct and erroneous trials should be observed.

The authors also show U-shape relationships between SAT conditions and SD over mean RT ratio and the skewness of RT distributions. Experimental data were fitted with the drift-diffusion model (DDM), and it was shown that DDM could not replicate the observed patterns under the threshold-tuning hypothesis. In response to the Rafiei and Rahnev experiment, Ratcliff and Kang developed a mixture model incorporating DDM with random fast guesses represented by a normal distribution with fixed mean and standard deviation (Ratcliff and Kang, 2021). The model was shown to fit the data from the experiment. The uncovered non-linear relationships pose a challenging task for decision-making models, and the authors suggest using the results as a validation test for decision-making models. However, this relationships can also shed light on how the SAT mechanism is implemented in the brain.

2. Results

In this section, I analyze the results of Rafiei and Rahnev's (2021) experiment with the decision-making model based on the recurrent attractor network with binary neurons (Penconek, 2020). I consider alternative computational mechanisms of SAT and show that the results of model simulations depend on the assumed mechanism, thus allowing to distinguish between them.

As suggested by Standage and colleagues (2014), the alternative ways of implementing speed-accuracy tradeoff can be linked to three main groups: (1) modulation of evidence encoding, (2) modulation of the integration of encoded evidence, and (3) modulation of the amount of integrated evidence sufficient to make a choice. In the context of the potential computational mechanism of SAT, I will thus consider three possibilities: (1) modulation of inputs (such as an urgency signal) which I will refer to as

the Evidence Encoding Hypothesis, (2) modulation of the control parameters responsible for the excitability of neurons in the choice circuit which I will refer to as the Gain Modulation Hypothesis, and (3) modulation of the decision threshold which I will refer to as the Threshold-Tuning Hypothesis. The effects of the two key alternative hypotheses: the gain modulation hypothesis and the threshold-tuning hypothesis are illustrated in Figure 1.

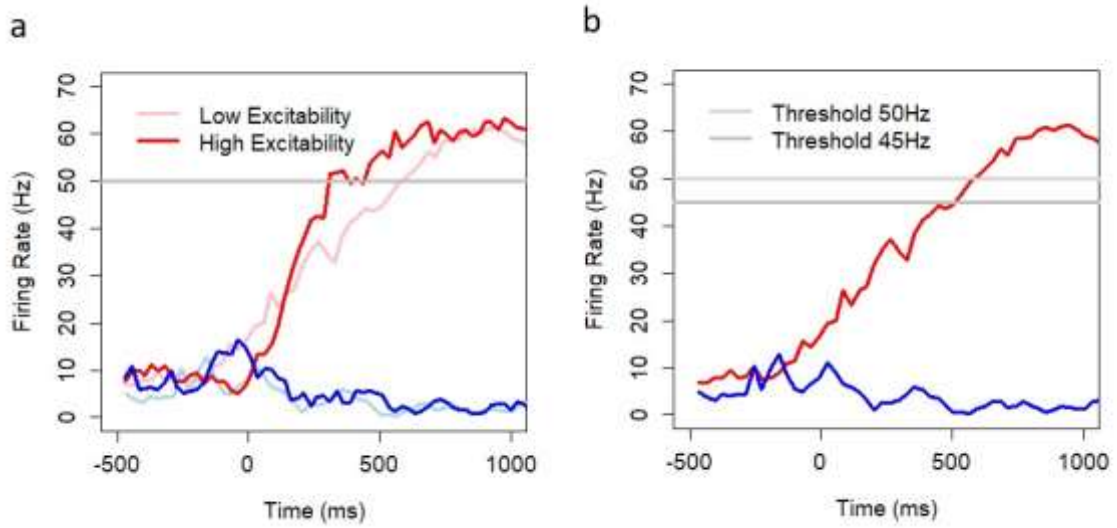

Figure 1. Effects of modulation of the excitability level (a) and the decision threshold (b) on the results of the accumulation-to-the-bound decision process.

Well-documented non-linearity of the neuronal integration process (Rolls, 2014; Peixoto et al., 2021) suggests that the effects of each type of modulation can be different. Intuitively, while changes to inputs and the parameters controlling the excitability of neurons are likely to rescale the neuronal integration process without affecting its intrinsic properties, changes to the decision threshold lead to termination of the process before it reaches the plateau of the decision state. Since the integration process is non-linear, its intrinsic properties can be affected by terminating it before it reaches the decision state. As we shall see, one of such properties is the ability of the decision system to produce negative RT difference, i.e., the shorter reaction time on correct responses than on erroneous responses.

Let us start with the threshold-tuning hypothesis and show that the results of model simulations based on this hypothesis are qualitatively consistent with experimental data.

Threshold-Tuning Hypothesis was modeled by assuming the linear relationship between stimulus and inputs to the decision system. The model was simulated with the Poisson inputs λ_A and λ_B (sampled each 30ms) dependent on the contrast level c = 4.98%, 6.39%, 8.21%, 10.54%, 13.53%:

$$\lambda_A = \lambda_0(\frac{1}{2} + c)$$

$$\lambda_B = \lambda_0(\frac{1}{2} - c)$$

where $\lambda_0 = 15$. Inputs reflect both the evidence in favor of each direction (i.e., +45 or -45 degrees) and against which are assumed to be provided by sensory neurons specific to each of these directions. For simplifying the computational experiment, stronger evidence is always provided to decision set A. Results are based on N= 15000 simulations (3000 per contrast level) with the standard values of control parameters. I consider threshold values in the range of 20 – 50Hz consistent with the fuzzy borders of model attractor states. The threshold is set based on the population-average firing rate in the winning decision pool of neurons (i.e., regardless of the firing rate in the dominated pool). The firing rate was calculated based on 30ms lags sampled each 10ms. Each model simulation started with 1000ms of spontaneous model run before stimulus onset. No decisions and decisions that took longer than 2000ms were removed for calculating the relationship between mean reaction time and accuracy (d') and the analysis of RT difference (Rafiei and Rahnev restricted the decisions to 1500ms). No restriction to 2000ms was used for calculating the SD/Mean RT ratio and the skewness of RT distributions. No non-decision time was assumed.

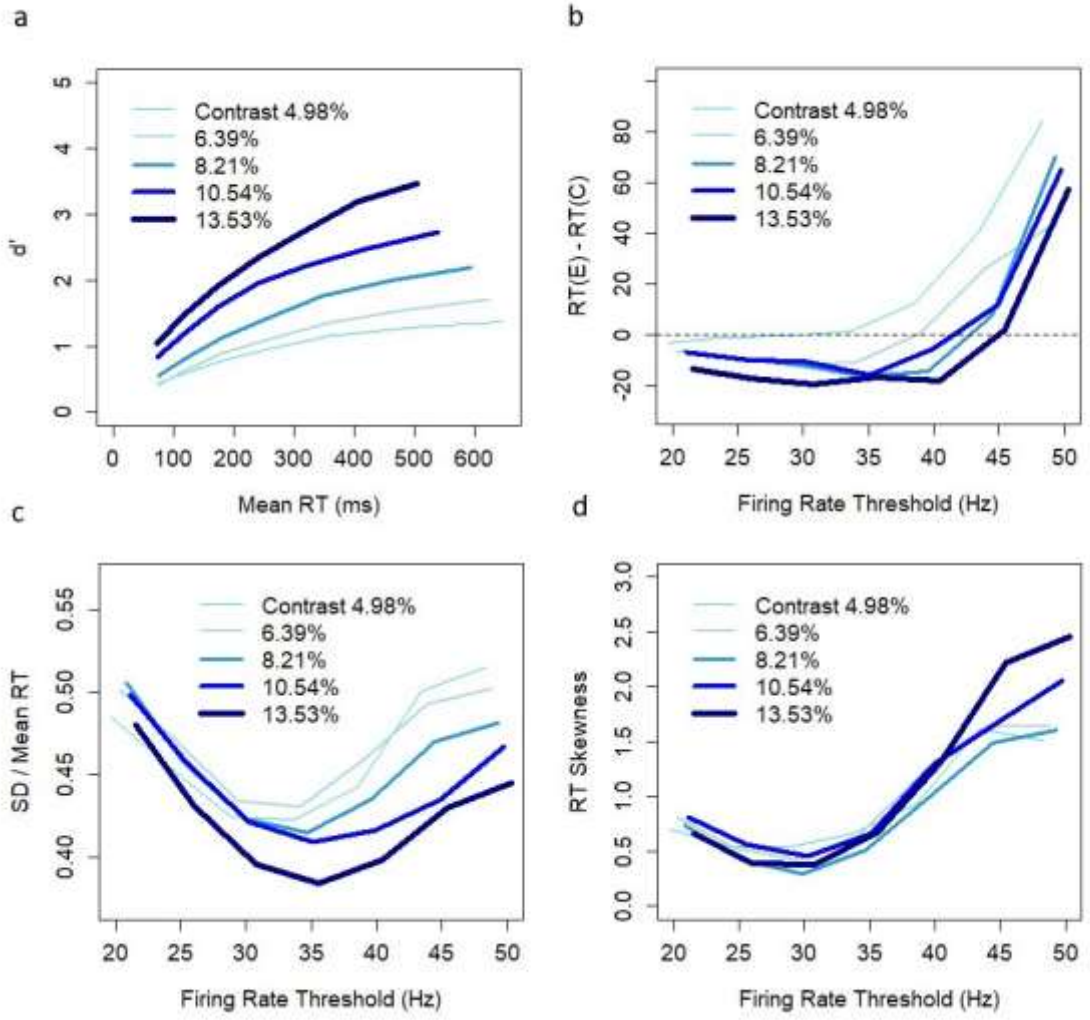

Figure 2. Model predictions based on N=15000 simulations (3000 per contrast level) with SAT effects implemented through population-average firing rate threshold (20-50Hz); A. Speed accuracy (d') tradeoff for five contrast levels (4.98% – 13.53%); B. Difference between RT (ms) on erroneous and correct decisions as a function firing rate threshold (range: 15-50Hz) in the winning attractor; C. Ratio between standard deviation and mean RT; D. Skewness of the RT distribution. No non-decision constant was assumed.

Results of model simulations are qualitatively consistent with the experimental data (Fig. 2). Relationships between reaction time and accuracy (d') reflect manipulations in the SAT conditions achieved in the experiment confirming the choice of latent values λ_A and λ_B (Fig. 2a). Note that for the lowest threshold value (20Hz), the model produces shorter RTs (in the range of 100ms and less) than observed experimentally (roughly 275ms). In order to avoid arbitrary improvement of the estimates, I have not assumed any non-decision time. Note that non-decision time is typically used in behavioral experiments and its justification assumes that an additional time is needed to encode sensory evidence

and to execute an action. Non-decision time has no impact on RT difference between correct and erroneous decisions, standard deviation and the skewness of RT distributions. However, it affects the mean RT and thus helps improve model fit with data.

The model produces negative RT difference with low frequency thresholds (20-35Hz) across all contrast levels (except the lowest contrast). The difference in reaction times between erroneous and correct decisions is statistically significant (Welsh Two Sample T-test, t = -4.8929, df = 2778.6, p = 1.05e-06; t = -4.2291, df = 2304.7, p = 2.437e-05; t = -3.8671, df = 1827.8, p = 0.000114 for contrast value 6.39% and thresholds: 20, 25, 30Hz respectively; t = -4.5659, df = 2391.1, p = 5.225e-06; t = -4.2969, df = 1851.4, p = 1.822e-05; t = -3.7441, df = 1418.4, p = 0.0001883; t = -3.3934, df = 1074.4, p = 0.0007155 for contrast value 8.21% and thresholds: 20, 25, 30 and 35Hz respectively; t = -4.7239, df = 1944.1, p = 2.479e-06; t = -4.2299, df = 1351.2, p = 2.496e-05; t = -2.8411, df = 873.76, p = 0.004601; t = -2.7882, df = 618.26, p = 0.005463 for contrast value 10.54% and thresholds: 20, 25, 30 and 35 respectively; t = -10, df = 1776, p < 2.2e-16; t = -7.4382, df = 1059.8, p = 2.103e-13; t = -5.1551, df = 655.81, p = 3.36e-07; t = -2.6733, df = 426.39, p = 0.007798 for contrast level 13.53% and thresholds: 20, 25, 30 and 35Hz respectively). The U-shape relationship is retrieved as the difference approaches zero with the lowest SAT levels (Fig. 2b). Both, the relationship between the frequency thresholds and SD over mean RT ratio and the frequency thresholds and the skewness of RT distributions form U-shape patterns (Fig. 2c and 2d) consistent with the experimental results.

Other hypotheses assume that the threshold value is hard-wired and fixed (at least in the range of time periods shorter than synapse plasticity latency). The fitness maximization principle suggests that the threshold value should allow the decision system to achieve maximum accuracy. Any value below the threshold associated with maximal accuracy permanently impairs the animal's ability to make correct decisions. This suggests that the threshold should fall within the basin of attraction of the decision state. However, the borders of basin of attraction sets are fuzzy (Methods, Fig. 8b). Initial conditions with a firing rate below 45-50Hz can still lead to convergence to the spontaneous state, and the system keeps improving the accuracy along with higher threshold levels. This excludes threshold values below

50Hz and suggests that the threshold should fall into the decision state. The reasonable choice of the threshold aligns it with the effective lower border of the decision state, i.e., 50Hz, as any higher threshold leads to longer reaction times with diminishing further improvement of accuracy.

Evidence Encoding Hypothesis: Let us now consider the hypothesis that SAT is controlled by changes in the inputs (such as an urgency signal provided simultaneously to both decision pools). If this hypothesis is true, the system should be able to produce a negative RT difference between erroneous and correct decisions for some range of input values. This is not the case. Reaction time on errors is longer than reaction time on correct decisions for the full range of inputs to the decision system.

The conclusion is based on the Monte Carlo analysis of N=20000 model simulations with random uniformly distributed values of the Poisson parameters of λ_A and λ_B in the range from 0 to 20. The model was simulated with the standard values of control parameters and threshold value 50Hz.

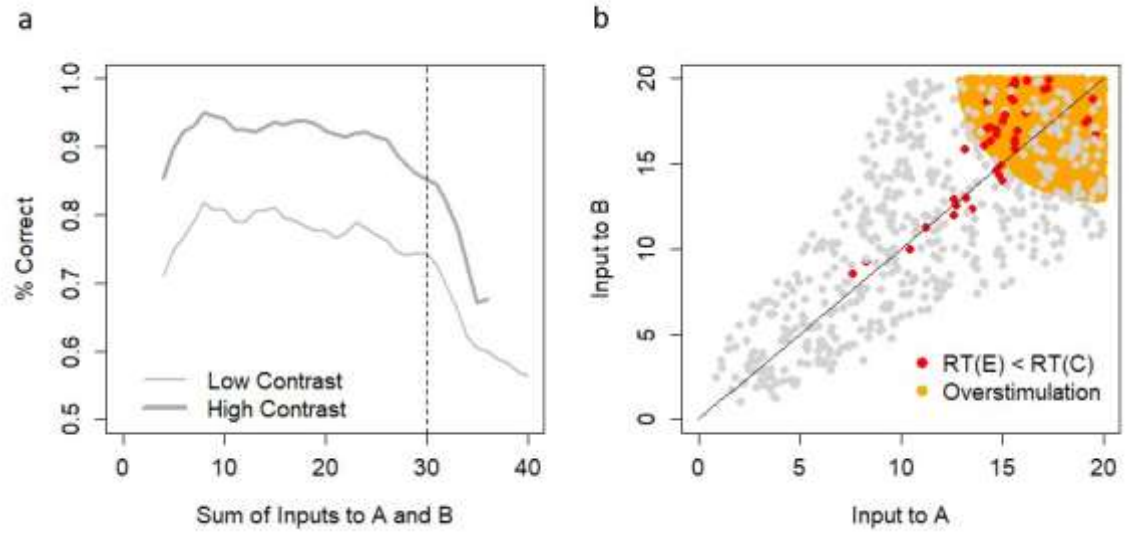

Figure 3. Model predictions based on N=20000 simulations with random values of Poisson inputs with parameter values λ_A and λ_B in the range 0-20. a. Correct Decisions as a function of the sum of inputs; b. RT difference between erroneous and correct decisions based on Monte Carlo analysis of the input space. Grey dots indicate the neighborhood when RT on errors is longer than RT on correct decisions. Red dots indicate the neighborhood when the opposite holds. The point is reported, if there are at least 50 instances of erroneous decisions in its neighborhood (as lower number of errors does not ensure enough stability).

Notice that the model saturates with a high sum of input values. The percentage of correct decisions drops when the sum of inputs exceeds 30 (Fig. 3a). Hence, a high sum of inputs can lead to overstimulation of the model. RT difference was tested by choosing a random point on the input space (uniform distribution) and selecting simulations with input parameters in the neighborhood of this point. Instances when RT on correct decisions is shorter than RT on errors align with the diagonal where the difference is close to zero or are located in the overstimulation zone (Fig. 3b). Otherwise, the model produces longer RT on erroneous than correct decisions. This excludes the possibility of replicating the experimental results with any SAT mechanism based on modulation of inputs (including modulation based on an urgency signal).

Gain Modulation Hypothesis assumes that the threshold firing rate is hard-wired and fixed while the SAT is controlled through top-down control signal projecting non-selectively to sensory-encoding and integrator populations. This signal increases the excitability of neurons in the choice circuit, which increases the baseline firing rate and the speed of evidence integration (Standage et al, 2014). Since changes in sensory-encoding cannot produce negative RT difference between erroneous and correct decisions, I will focus on considering changes that affect the excitability of neurons in the choice circuit. The excitability of the network in the model is controlled by the inhibition constant Θ, which sets the normative level of neuronal excitation ($\Theta = 0.13$). The increase of the inhibition constant ($\Theta > 0.13$) increases the level of neuronal excitation and is associated with the "speed" condition, while the decrease is associated with the "accuracy" condition. The domain of the parameter is the interval (0.1, 0.2) and is related to the chosen proportion of neurons in the decision sets in the network (i.e., 10%). Inhibition levels below 0.1 result in restricting the possibility of all neurons in the decision set to be active at the same time. Inhibition levels above 0.2 can lead to violating the winner-take-all property as it allows for neurons in both decision sets to be active at the same time.

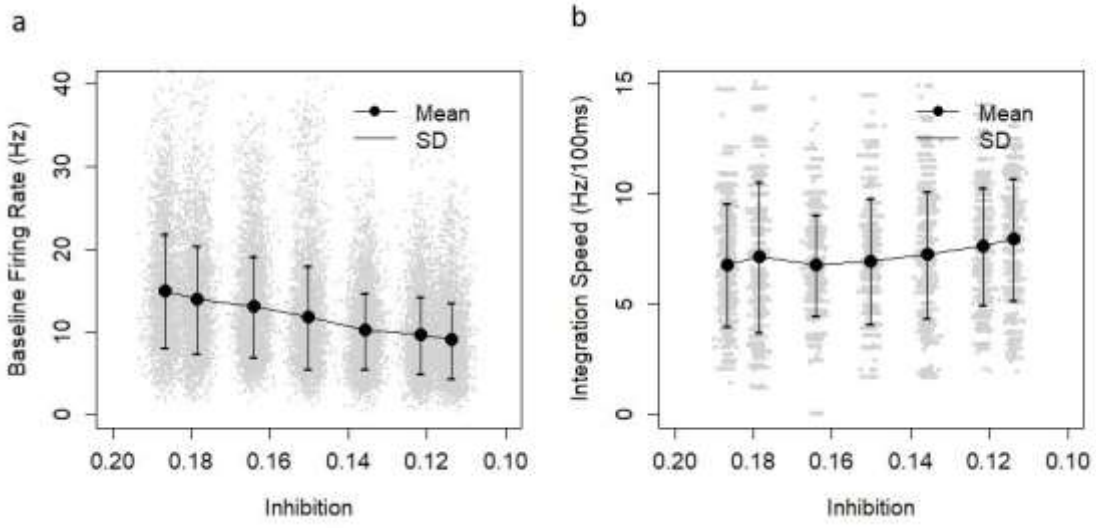

Figure 4: Effects of the manipulation of the inhibition constant; A. Baseline Firing Rate (Hz): average in the decision set during the spontaneous run; B. Integration Speed (Hz/100ms): average based N = 7000 model runs with random contrast levels: 4.98% - 13.53% (i.e., N = 1000 per inhibition level).

Manipulations of the inhibition constant ($0.1 < \Theta < 0.2$) lead to changes of the baseline firing rate in the decision set in the spontaneous state that are consistent with the mechanism postulated by the gain modulation hypothesis (Fig. 4a). The average baseline firing rate is 9Hz (SD = 4.6) in the "accuracy" condition ($\Theta = 0.11$) and increases to 15Hz (SD = 6.9) in the "speed" condition ($\Theta = 0.19$). The relationship is significant (ANOVA, $F = 3025.9$, $df = 1$, $p < 2.2e\text{-}16$). Increase of inhibition constant decreases reaction time (RT), but does not increase the integration speed (Fig. 4b). The average speed of integration is 8Hz/100ms (SD = 2.8) in the "accuracy" condition ($\Theta = 0.11$) and decreases to 6.8Hz/100ms (SD = 2.8) in the "speed" condition ($\Theta = 0.19$). The relationship is significant (ANOVA, $F = 92.3$, $df = 1$, $p < 2.2e\text{-}16$). The above result are based on 7000 simulations with random values of contrast in the range 4.98% to 13.53% (uniform distribution).

In order to understand the impact of inhibition constant on SAT effects, I conducted N= 40000 simulations (8000 per contrast level) with the random values of the inhibition constant Θ in the range 0.1 to 0.2 (uniformly distributed) and the standard values of other control parameters. In line with the gain modulation hypothesis, which postulates hard-wired threshold, the threshold was fixed and set

at the value of 50Hz (border of the decision set). I assumed the same linear relationship between stimulus and Poisson inputs λ_A and λ_B and model settings as in the threshold-tuning hypothesis.

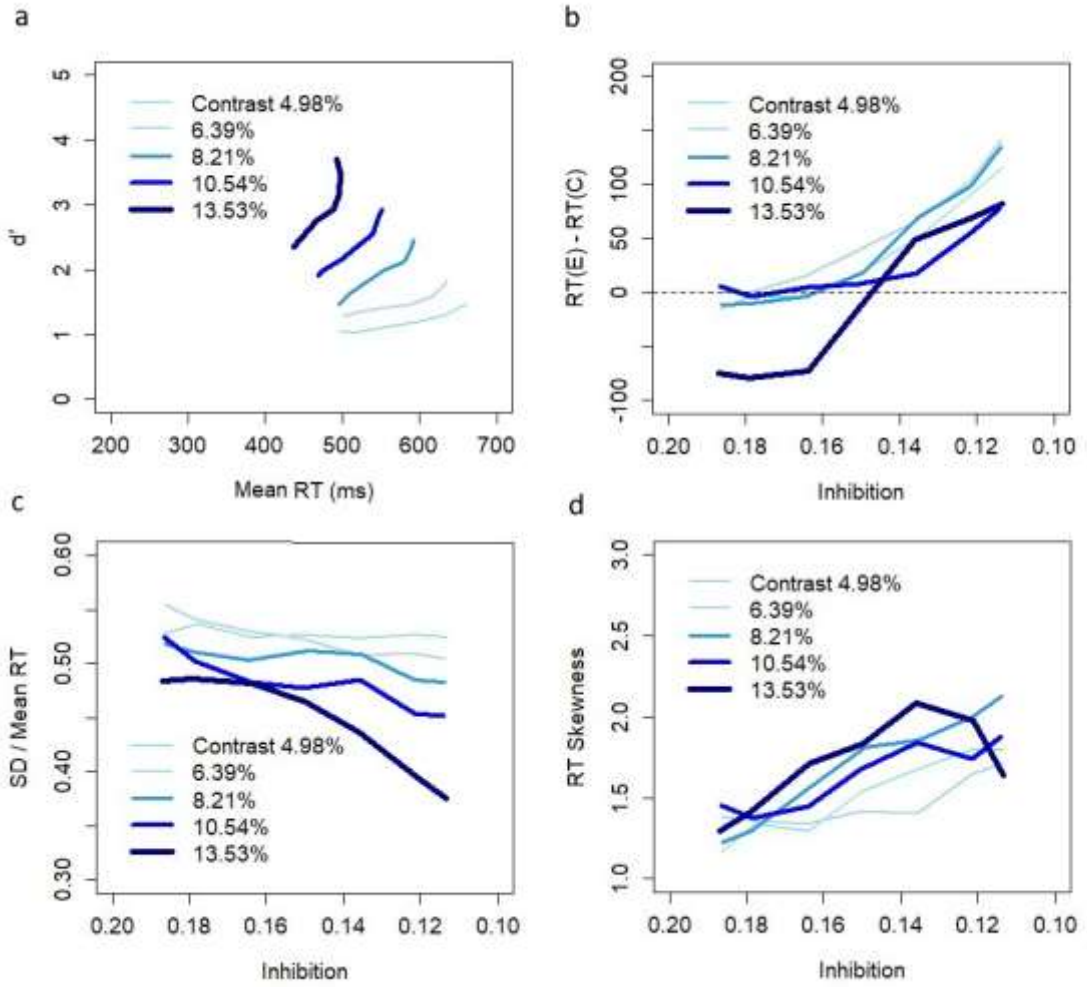

Figure 5: Model predictions based on N=40000 simulations (8000 per contrast level) with SAT effects implemented through manipulation of the inhibition constant (0.1 – 0.2). Higher inhibition constant indicates higher excitability of neurons in the system and thus is associated with the "speed" condition; A. Speed accuracy (d') tradeoff for five contrast levels (4.98% – 13.53%); B. Difference between RT (ms) on erroneous and correct decisions as a function inhibition constant (0.1 - 0.2); C. Ratio between standard deviation and mean RT; D. Skewness of the RT distribution. No non-decision constant was assumed.

Changes in the inhibition constant create SAT effects (Fig. 5a) across all contrast levels. The average RT is 492ms (SEM: 0.15) in the "accuracy" condition (Θ = 0.11) and 436ms (SEM: 0.16) in the "speed" condition for the highest contrast (13.53%) while d' decreases from 3.7 to 2.4. For the median contrast (8.21%), RT decreases from 591ms (SEM: 0.18) to 496ms (SEM: 0.18) and d' from 2.5 to 1.5 in the "accuracy" and "speed" conditions, respectively. However, the patterns of SAT effects are not

consistent with the experimental data. First, the magnitude of the effect on average RT is much smaller than observed experimentally. In the experiment, RT decreased from roughly 575ms in the “accuracy” condition to roughly 275ms in the “speed” condition for the median contrast. Second, there are no negative RT differences between RT on errors and correct decisions except the highest contrast (the highest absolute t-value = 1.4203, df = 201.05; p = 0.1571 in T-test across contrast levels: 6.39%, 8.21%, 10.54% and inhibition levels: 0.16, 0.18 and 0.19). Third, there is no evidence of U-shape relationships neither for RT difference (Fig. 5b) nor for SD/Mean RT ratio (Fig. 5c) nor for the skewness of RT distributions (Fig. 5d). Hence, the hypothesis that the computational mechanism behind the SAT relies on the modulation of neuronal excitability in the choice circuit affecting the baseline firing rate and the speed of the integration process is inconsistent with the experiment. This makes us reject the gain modulation hypothesis based on the model.

Note that at least one of the counterarguments against the gain modulation hypothesis is general and applicable to a wider class of decision-making models. Suppose modulation of the baseline firing rate preserves the intrinsic properties of the integration process, and a decision-making model always produces a positive RT difference between errors and correct decisions regardless of inputs. In that case, modulation of the baseline firing rate cannot produce negative RT difference either, and hence model simulations would be inconsistent with the experiment. In particular, Wang's attractor network model was shown to produce slower mean decision times on erroneous trials than correct trials (Wong and Wang, 2006; Standage et al., 2011).

In this context, it is surprising to see the negative RT difference for the highest contrast in the discussed results (Fig. 5b). It was checked that the effect relates to a displacement of the decision state. Apparently, the borders of decision states are not constant. They become less coherent due to changes in the inhibition constant and move with the strength of inputs.

The above analysis provides support for the threshold tuning hypothesis. However, it does not resolve the controversy with neurophysiologic observations, which show a higher level of baseline firing rates

and a higher speed of neuronal integration under "speed" condition (van Veen et al., 2008; Ivanoff et al., 2008; Forstmann et al., 2008; Hanks et al., 2014; Heitz and Shall, 2012). If these effects are not responsible for SAT, they are related to other neuronal mechanisms interfering with SAT. In the last part of the paper, I investigate the effects of desynchronization of alpha oscillations on the decision process. The purpose of this section is not to provide the explanation of the desynchronization mechanism itself, but to show that alpha oscillations interact with the SAT mechanism and this interaction provides an alternative explanation of why the increase of the baseline firing rate and the speed of evidence integration is observed during the speed condition. These investigations allow us to reconcile the threshold-tuning hypothesis with the neurophysiological observations which are considered the key supporting evidence for the gain modulation hypothesis.

Interference with alpha waves: Growing body of research shows that alpha oscillations interfere with the decision process and behavioral performance. Presentation of a stimulus leads to desynchronization of alpha oscillations (event-related desynchronization) followed by alpha power increase after task execution (Klimesch et al., 2006). Magnitude and timing of alpha waves suppression and resynchronization depend on the task type, duration, and difficulty. Large reference alpha power during the anticipation period is positively correlated with performance (Vogt et al., 1998; Klimesch et al., 2000; Doppelmeyr et al., 2002) and is negatively correlated with decision time (Paluch et al, 2021). However, the effect might depend on task difficulty: longer decision time for an easy task and lower rate of erroneous responses in a difficult task (Kuc et al, 2021). Experiments on monkeys performing somatosensory discrimination tasks with a sequential presentation of stimuli indicate that the decrease of alpha power (in premotor and motor regions) correlates with better discrimination performance (Haegens et al., 2011). The same study shows that spike activity negatively correlates with alpha power and neuronal firing depends on the alpha phase. The link between metabolic activity and alpha power was reported in several studies (Goldman et al., 2002; Laufs et al., 2003a, b; Moosmann et al., 2003): increase of alpha power is related to a decrease in metabolic rate. However,

in some brain areas, the relation is reversed (Sadato et al., 1998; Goldman et al., 2002; Laufs et al., 2003a, b; Moosmann et al., 2003).

Model predictions: Following the suggestion from the study of Haegens and colleagues (Haegens et al., 2011), I designed a computational experiment in which alpha oscillations are implemented through the inhibitory mechanism. The mechanism is exogenous to the decision system and is introduced through time-dependent oscillatory modulation of the inhibition constant:

$$\theta = \theta_0 + A \sin(\omega t + \xi)$$

where $\theta_0 = 0.13$ is the baseline inhibition constant and A, ω and ξ are amplitude, frequency, and phase of alpha waves, respectively. Thus, neuronal excitability follows rhythmic changes over time. Whether a particular neuron is activated or not depends on the same update rule as before, except that the global threshold level is now time-dependent. I consider alpha oscillations in the frequency range of 8-12 Hz and amplitudes in the range 0-0.1. If A = 0.1, the inhibition constant varies over time between 0.03 and 0.23. Initial phase ξ is a random parameter (uniform distribution in the range 0-2π). Other control parameters are set at their standard values.

Introducing alpha oscillations does not compromise the fundamental properties of the model. The model keeps a persistent activity of the network, exhibits the emergent neuronal integration process (Fig. 6a), and facilitates winner-take-all competition between the decision states. The activity of the network shows characteristic phase dependencies with rhythmic increase and decrease of neuronal activity (Fig. 6b). Despite symmetric changes in relation to the baseline inhibition constant, the baseline firing rate in the spontaneous state decreases as a function of amplitude (Fig. 6c) from the mean value of 10.2 (SD = 4.8) to 10.3Hz (SD = 5) when the amplitude is 0 and 0.02 to 9.2Hz (SD = 2.7) and 8.9Hz (SD = 2.2) when the amplitude is 0.08 and 0.1 respectively. The decrease is statistically significant (ANOVA, F = 931.18, df = 1, p < 2.2e-16). Higher amplitudes also decrease the range of fluctuations of the network in the spontaneous state. Standard deviation is in the range of 4.8 and 5 for amplitude levels 0 and 0.02 and drops to 2.7 and 2.2 for amplitude levels 0.08 and 0.1. These results are consistent

with the experiments, which show a decrease of spike activity (Haegens et al., 2011) and metabolic rate (Goldman et al., 2002; Laufs et al., 2003a, b; Moosmann et al., 2003) with increased alpha power. Model predictions show a negative relationship between alpha oscillations and the speed of the integration process (Fig. 6d) in the amplitude range of 0.02 – 0.08. The average speed of integration for correct decisions is 7.9Hz (SD = 2.7) per 100ms for the amplitude of 0.02 and drops down to 5.3Hz (SD = 2.3) per 100ms for the amplitude of 0.08. The decrease is statistically significant (ANOVA, $F = 253.78$, $df = 1$, $p < 2.2e\text{-}16$). The analysis was conducted with random contrasts (uniform distribution) in the range of 4.98% - 13.53%. Simulations with correct decisions were selected from the set of N=3000 (500 per amplitude level) model simulations. The rate of no decisions was high for the amplitude level of 0.1, resulting in only 11 correct decisions out of 500 for the highest value of amplitude (0.1).

The model also predicts the interference effects between alpha oscillations and the discriminatory power, and the mean reaction time of the decision system. The analysis was conducted based on N=15000 model simulations for five contrast levels (3000 simulations per contrast). Alpha oscillations of random frequency in the range of 8-12Hz (uniform distribution), random amplitude in the range 0-0.1 (uniform distribution), and random initial phase (uniform distribution) were implemented. As before, I assumed the same linear relationship between stimulus and Poisson inputs λ_A and λ_B, and the standard model settings.

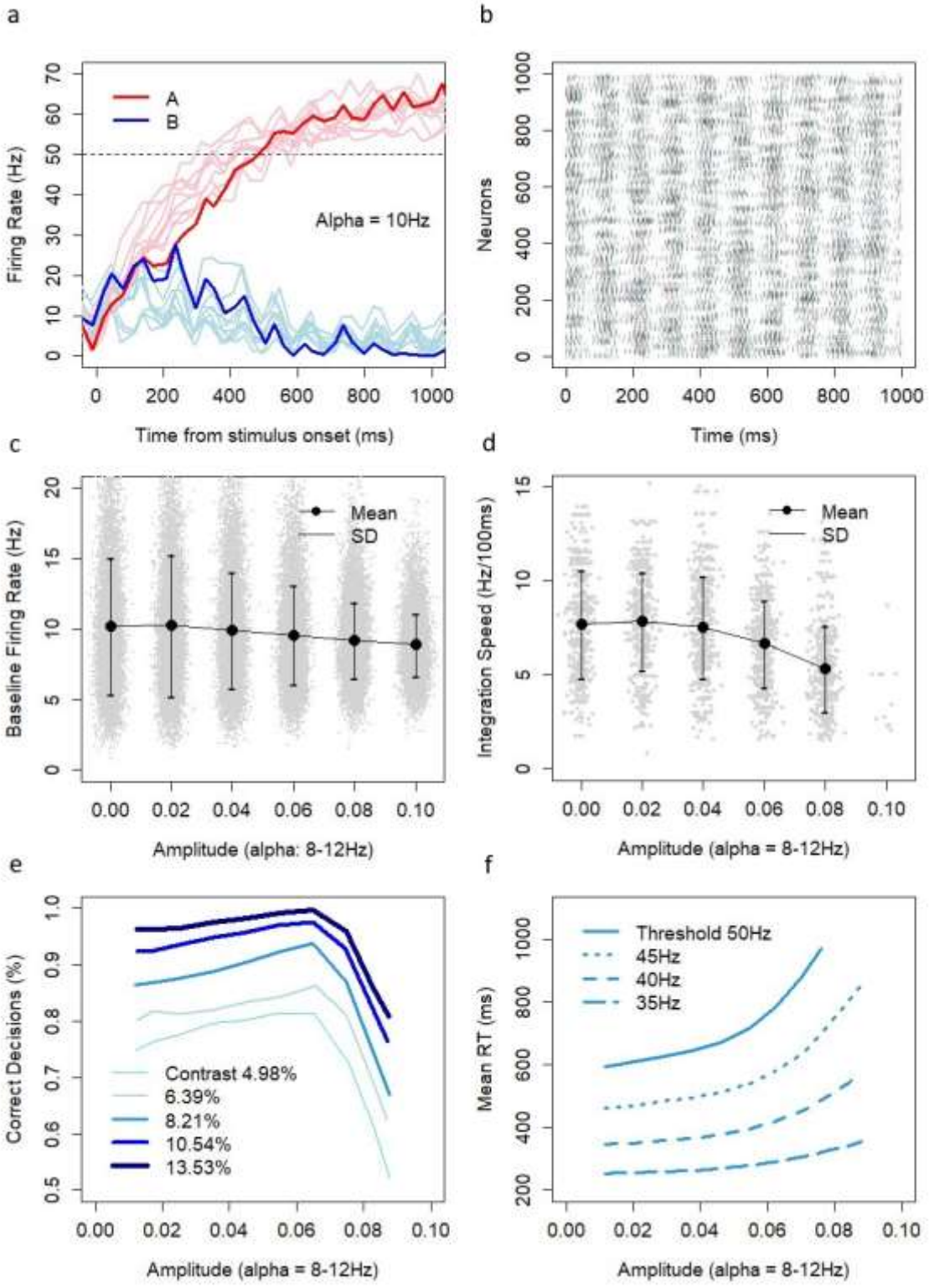

Figure 6: Interference between alpha oscillations (8-12Hz) and the decision process. a. Firing rate after stimulus onset in pools A and B for model runs with alpha oscillations (10Hz) and coherence level c = 51.2%; b. Spiking activity of neurons in the decision system during the spontaneous model run with alpha oscillations (10Hz). c. Baseline Firing Rate (Hz): average in the decision set during the spontaneous run with alpha oscillations of random frequency (8-12Hz), time bins 100ms; d. Integration Speed (Hz/100ms): average based N = 2351 model runs with alpha oscillations of random frequency

(8-12Hz) and random contrast levels: 4.98% - 13.53%, time bins 30ms; e. Discriminatory power as a function of the amplitude of alpha oscillations (8-12Hz) for different contrast levels and threshold 50Hz; f. Reaction Time (RT) as a function of the amplitude of alpha oscillations (8-12Hz) for different thresholds (35-50Hz) and medium contrast level 8.21%.

The model reveals an interesting relationship between the amplitude of alpha oscillations and the discriminatory power of the decision system. Figure 6e shows the percentage of correct decisions over 2500ms after stimulus onset with regard to all model runs as a function of amplitude for the threshold value of 50Hz and five contrast levels. For the amplitudes in the range of 0-0.06, the discriminatory power of the system increases. The relationship is significant (Probit Regression, est. = 12.7, t = 3.3273, p = 0.0008769; est. = 9.9, t = 3.4922, p = 0.0004791; est. = 7, t = 3.1492, p = 0.001637; est. = 6.5, t = 3.3897, p = 0.0006996 for contrast levels 13.53%, 10.54%, 8.21% and 4.98%, respectively), except contrast 6.39% (Probit Regression, est. = 3, t = 1.4631, p = 0.1434). The percentage of correct decisions reaches its peak at the amplitude in the range 0.05-0.06 (83.2% ± 2.2 SEM; 85.7% ± 2.1 SEM; 94.4 ± 1.3 SEM; 97.3% ± 0.9 SEM; 99.7% ± 0.3 SEM for contrast levels: 4.98%, 6.39%, 8.21%, 10.54%, 13.53%, respectively). This peak is higher versus the baseline scenario with no alpha oscillations for all contrast levels (75.1% ± 0.8 SEM; 80% ± 0.7 SEM; 86.2% ± 0.6 SEM; 91.3% ± 0.5 SEM; 95.7% ± 0.4 SEM). This is interesting. It shows that the existence of alpha oscillations can improve the discriminatory power of the decision system. This also explains why the psychometric function (Methods, Fig. 9a) derived from the model without alpha oscillations is less steep than observed in some experiments (Roitman and Shadlen, 2002). After the peak, the discriminatory power drops because of an increase in the percentage of no-decisions, i.e., with high amplitude levels, the sensitivity of the decision system to inputs decreases. For example, when the amplitude is in the range of 0.08 to 0.1, the system converges to a correct decision in 60% (± 2 SEM) of cases, makes an erroneous decision in <1% of cases (3/613), and makes no decision at all in 39% (± 2 SEM) of cases for the medium contrast 8.21%.

In the context of the negative impact of alpha power on the baseline firing rate and the speed of the integration process, it is not surprising to see the negative relationship between the amplitude of alpha oscillations and reaction time (Fig. 6f). For the threshold value of 50Hz and the median contrast level

8.21%, the mean RT increases from 595ms (± 11 SEM) for the initial interval with mean amplitude 0.011 (width ± 0.02) to 717ms (± 12 SEM) for the interval with mean amplitude 0.055 (width ± 0.02). The relationship over the amplitude range (0 – 0.06) is significant (ANOVA, F = 24.185, df = 1, p = 9.555e-07). For the threshold level of 40Hz and the median contrast level, the mean RT increases from 345ms (± 5 SEM) to 394ms (± 6 SEM) between intervals with mean amplitude 0.011 and 0.055. The relationship over the amplitude range (0 – 0.06) is significant (ANOVA, F = 15.194, df = 1, p = 0.0001006).

Reconciling the threshold-tuning hypothesis with neurophysiologic data: Analysis presented in this paper supports the threshold-tuning hypothesis of the SAT and provides counterarguments against the gain modulation hypothesis. The gain modulation hypothesis is supported by three neurophysiologic observations. First, the threshold firing rate of neurons measured experimentally is the same during "speed" and "accuracy" conditions. Second, the baseline firing rate of neurons is higher in the "speed" condition compared to the "accuracy" condition. Third, the speed of neuronal integration is faster during the "speed" condition compared to the "accuracy" condition.

First, let us notice that the implementation of the threshold-tuning hypothesis in terms of population-average firing rate in the decision pool is not inconsistent with the fixed threshold value for neurons in the pool. Neurons in the decision system exhibit phase transition between the low-frequency state (with the spike-count rate in the range of 10Hz) and the high-frequency state (with the spike-count rate 70Hz assumed in the model). However, this transition happens at various moments for different neurons (Methods, Fig. 8d). Thus, a lower threshold level implemented as the population-average firing rate is manifested by a lower coherence between firing rates of neurons in the decision pool, not by a lower firing rate of these neurons in the high state.

The interference of alpha waves with the decision process suggests that there is an optimal alpha amplitude level that enhances the decision system's discriminatory power over the baseline level without alpha oscillations. The fitness maximization principle implies that this amplitude of alpha

oscillations should be maintained in the “accuracy” condition. Conversely, alpha oscillations should be suppressed during the “speed” condition, as higher amplitude levels imply longer reaction time. Suppressing alpha power results in increased baseline firing rate and increased speed of neuronal integration, the effects observed experimentally during the “speed” condition (van Veen et al., 2008; Ivanoff et al., 2008; Forstmann et al., 2008; Hanks et al., 2014; Heitz and Shall, 2012). The interaction of alpha waves with the decision process explains the neurophysiologic data related to differences between “speed” and “accuracy” conditions.

3. Discussion

The behavioral experiment of Rafiei and Rahnev (2021) shows robust U-shape patterns with regard to RT difference between erroneous and correct decisions, the SD over mean RT ratio, and RT skewness as a function of SAT conditions. Computational analysis conducted through the recurrent attractor network decision-making model with binary neurons reveals that these patterns are consistent with the threshold-tuning hypothesis of the SAT and are inconsistent with alternative hypotheses, which assume the threshold level is hard-wired. In particular, these patterns are inconsistent with the gain modulation hypothesis (Standage et al, 2014). At least part of the counterargument against the gain modulation hypothesis is general and applicable to a wider class of decision-making models (including Wang's model) which show a longer reaction time on erroneous decisions than correct ones. Thus, the rejection of the gain modulation hypothesis is not model-specific.

The gain modulation hypothesis is supported by neurophysiological observations that show that neurons' baseline firing rate is higher, and the speed of neuronal integration is faster during the "speed" than the "accuracy" condition. These effects are explained by the interference of alpha waves (8-12Hz) with the decision process. In the “accuracy” condition, alpha oscillations are maintained to enhance the discriminatory power of the decision system. In the “speed” condition, alpha oscillations are suppressed to increase reaction time. On the neuronal level, suppressing alpha oscillations leads

to an increase of the baseline firing rate and the speed of neuronal integration, neurophysiological effects observed experimentally.

The question of how the threshold-tuning hypothesis is mechanistically implemented in neural circuits is open. Under the threshold-tuning hypothesis speed-accuracy tradeoff is an inference problem: whether the ongoing neuronal integration process will eventually converge to a decision state. Influential papers (Gold and Shadlen, 2002; Bogacz et al., 2006) provide compelling arguments in favor of the thesis that the brain uses integration to the bound process to solve such inference problems. If so, the inference problem of the SAT might be mechanistically implemented as a downstream parallel evidence integration process. Such a downstream parallel process was discovered in the superior colliculus. Inputs to the downstream integration process are gated through tonic inhibition in basal ganglia. One can hypothesize that the threshold is set by the gating inhibition level in basal ganglia. This is a plausible hypothesis in the context of the fact that SAT effects are observed among various species, including rodents and insects. Why are there two separate neuronal integration processes? The first process located in the lateral intraparietal (LIP) area is the decision process about the incoming evidence from the environment. The second process located in the superior colliculus triggers a behavioral response and thus is responsible for the subsequent decision of whether and when to react to the stimulus. Further research is necessary to prove or disprove these ideas.

The model presented in this paper is consistent with neurophysiological observations and is capable of replicating dot motion discrimination experiments (Shadlen and Newsome, 2001; Roitman and Shadlen, 2002). The behavioral experiment of Rafiei and Rahnev (2021) is considered by its authors a demanding task for decision-making models. The model under the threshold-tuning hypothesis is capable of producing predictions consistent with the patterns achieved in the experiment. The model also produces testable predictions such as the optimal amplitude of alpha oscillations that enhance the decision system's discriminatory power. I hope these predictions can be investigated in future experimental research and support or falsify the proposed modeling approach. None of the alternative decision-making models (including DDM and Wang's model) can handle the full scope of analysis

presented in this paper. The analysis suggests that the interference of the decision process with alpha waves is a non-negligible factor. Future experimental studies and modeling approaches should account for this interference.

Methods

Results presented in this paper were obtained in silico through the attractor network model with binary neurons (Penconek, 2020). Last two decades of neurophysiologic and theoretical research (Newsome, Britten and Movshon, 1989; Britten et al, 1992; Shadlen and Newsome, 2001; Riotman and Shadlen, 2002, Gold and Shadlen, 2002; Kable and Glimcher, 2009; Wang, 2002; Wong and Wang, 2006; Rolls, 2014) has led to establishing the paradigm of how decision-making for the two-alternative forced-choice task is implemented in the brain. The neural circuit computing a categorical decision is the recurrent network with a global inhibition which facilitates winner-take-all competition between the attractors. Wang developed the mechanistic implementation of a decision-making circuit with leaky integrate-and-fire neurons (2002). An alternative implementation of the circuit with binary neurons (Penconek, 2020), considered in this paper, is based on the following four phenomenological assumptions:

Neurons integrate inputs from their presynaptic connections, and when the threshold is reached, they fire an action potential and stay inactive over the refractory period. In the model, a binary state is assigned to each neuron (N = 1000) at time t: $s_t(\mathrm{i}) = 1$ if the neuron is in the refractory period and 0 otherwise. Spike is emitted each time the neuron is updated to state $s_t(\mathrm{i}) = 1$. A neuron is "active" at time t iff $s_t(\mathrm{i}) = 1$. For simplicity of implementation, I assume that the length of the effective refractory period is the same as the synapse constant d, i.e., the time of integrating inputs. In this convention, the excitatory input from presynaptic neurons is given by:

$$\int_{t-d}^{t} \sum_{j=1}^{N} \delta(\tau - t_k(j))\, w_{ij}\, d\tau \;\; = \sum_{j=1}^{N} \; s_t(\mathrm{j})\, w_{ij}$$

where $t_k(j), k = 1, 2 \ldots$ is the sequence of times at which spikes occurred in the presynaptic neuron j and w_{ij} $(j = 1\ to\ N)$ are the presynaptic connections of the neuron i. Connections are random and binary that is $w_{ij} = 0$ or 1. No restrictions on the connections are imposed. In particular, the network is not assumed to be symmetric.

Global inhibition ensures the stability of the network with a balance between excitation and inhibition and facilitates winner-take-all competition between decision states. The global inhibition is implemented through the common inhibitory threshold in the model. With balanced excitation and inhibition, the threshold is a function of the activity of excitatory neurons, and the model can be reduced to excitatory neurons only. I postulate that the threshold is set in relative terms and varies with the square of the proportion of active neurons during the update time, i.e., the update rule is given by:

$$s_t(\mathrm{i}) = \; 1 \text{ iff } \; \frac{\sum_{j=1}^{N} s_t(\mathrm{j})\, w_{ij}}{\sum_{j=1}^{N} w_{ij}} > \frac{1}{\Theta} \cdot \left(\frac{\sum_{j=1}^{N} \; s_t(\mathrm{j})}{N} \right)^2$$

where Θ is the inhibitory constant (Θ = 0.13) which defines the normative excitation level of neurons in the system. The proposed update rule ensures a persistent activity of the network with no exogenous stochastic stimulation, provided the initial state of the network is non-zero. The model is initialized with random non-zero states with probability Θ.

Asynchronous evolution of the network follows the Poisson point process (Dayan and Abbott, 2001; Wójcik, 2018), i.e., time intervals between consecutive updates are distributed exponentially with the rate λ_2 $(\lambda_2 = 0.006)$ except for the constant refractory periods $1/\lambda_1 \sim 14{,}3\mathrm{ms}$ $(\lambda_1 = 0.07)$; the latter sets the maximum firing rate (70Hz) of neurons in the model (as suggested in Rolls, 2014). Note that the assumed refractory period is longer than the observed refractory period of neurons in vivo. The

assumed constant relates to the effective time interval between two consecutive spikes emitted by neurons when they fire with the maximum firing rate.

Network architecture consists of three pools of neurons: two decision pools, A and B (each n = 100), with a higher density of random connections within each set d_1 ($d_1 = 0.55$) and the rest of the network (Fig. 7). Connections in the rest of the network and between different pools of neurons have density d_2 ($d_2 = 0.36$). A higher density of connections in the decision pools is assumed to be a result of Hebbian learning (Hebb, 1949); no learning mechanism is introduced in the model. Connections are regenerated before each model simulation and are kept constant during a simulation.

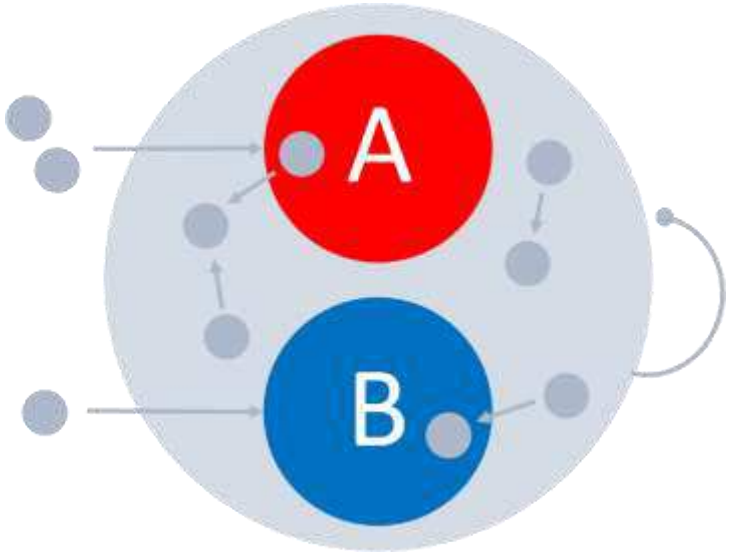

Figure 7: Network architecture of the decision system: the recurrent network of the excitatory neurons with a higher density of connections in neuronal pools A and B. Neuronal pools A and B form the decision sets and are selective to inputs. Inputs are provided by separate pools of neurons (outside of the decision system) projecting to A and B, respectively. The system is equipped with the global inhibition mechanism facilitating winner-take-all competition.

The decision sets A and B are selective to inputs. Consistent with the structure of the model, inputs are provided by two pools of additional neurons (up to 20) to 50% of neurons in A and B, respectively. Input pools form additional presynaptic connections, and their activity modifies the excitatory input of neurons in A and B. Input values are latent variables and are provided to the decision system by sensory encoding neurons reacting to stimulus. The strength of inputs is assumed to be directly related to the stimulus (linear relationship). The strength of inputs is controlled by the time-variable sequence of

active neurons encoding the evidence in favor of each decision alternative. The sequence (of natural numbers) is derived from the Poisson distribution (Poisson inputs) with the parameters λ_A and λ_B reflecting the strength of the evidence in favor of decisions A and B, respectively. Alternatively, inputs can be non-random and provided by time-constant real values modifying the excitatory input to neurons in A and B. Non-random inputs are not biophysically realistic, but they produce results equivalent to those with the Poisson inputs.

The model has several control parameters: the size of network (N = 1000) and pools A, B (n = 100 each), the inhibitory constant ($\theta = 0.13$), parameters controlling time evolution of the network ($\lambda_1 = 0.07$ and $\lambda_2 = 0.006$) and the density constants ($d_1 = 0.55$ and $d_2 = 0.36$). The control parameters are responsible for the emergent attractor dynamics of the system. Some model parameters are arbitrary (its overall size and sizes of the decision pools A and B). For the inhibition mechanism to facilitate winner-take-all completion, the value of the inhibition constant θ falls into the range from 0.1 to 0.2. Parameter $\lambda_1 = 0.07$ defines the maximum frequency of spikes (70Hz). This value is consistent with the maximum firing rate of LIP neurons in the human brain (Rolls, 2014). In the version of the model considered in this paper, we assign a constant time $1/\lambda_1 \sim 14{,}3\text{ms}$ to neurons in the refractory period, while in the previously presented version (Penconek, 2020), the refractory period was assumed to be random (exponential distribution with parameter λ_1. It was checked that both choices lead to the same emergent dynamics and comparable model performance. Parameter λ_2 $(\lambda_2 = 0.006)$ controls the speed of neuronal integration and was set experimentally in order for the model to produce biophysically realistic reaction times (in the range of hundreds ms).

With other parameters (N, n, θ, λ_1, and λ_2) set, the model works only under a particular and narrow range of the density ratio d_1/d_2 (Penconek, 2020). If the ratio is greater than this value, the model becomes unstable and converges to a decision within a short amount of time with no inputs provided. If the ratio is smaller than this value, the model becomes insensitive to inputs and maintains the spontaneous state despite inputs. The control parameters are fixed at their default values if not stated otherwise.

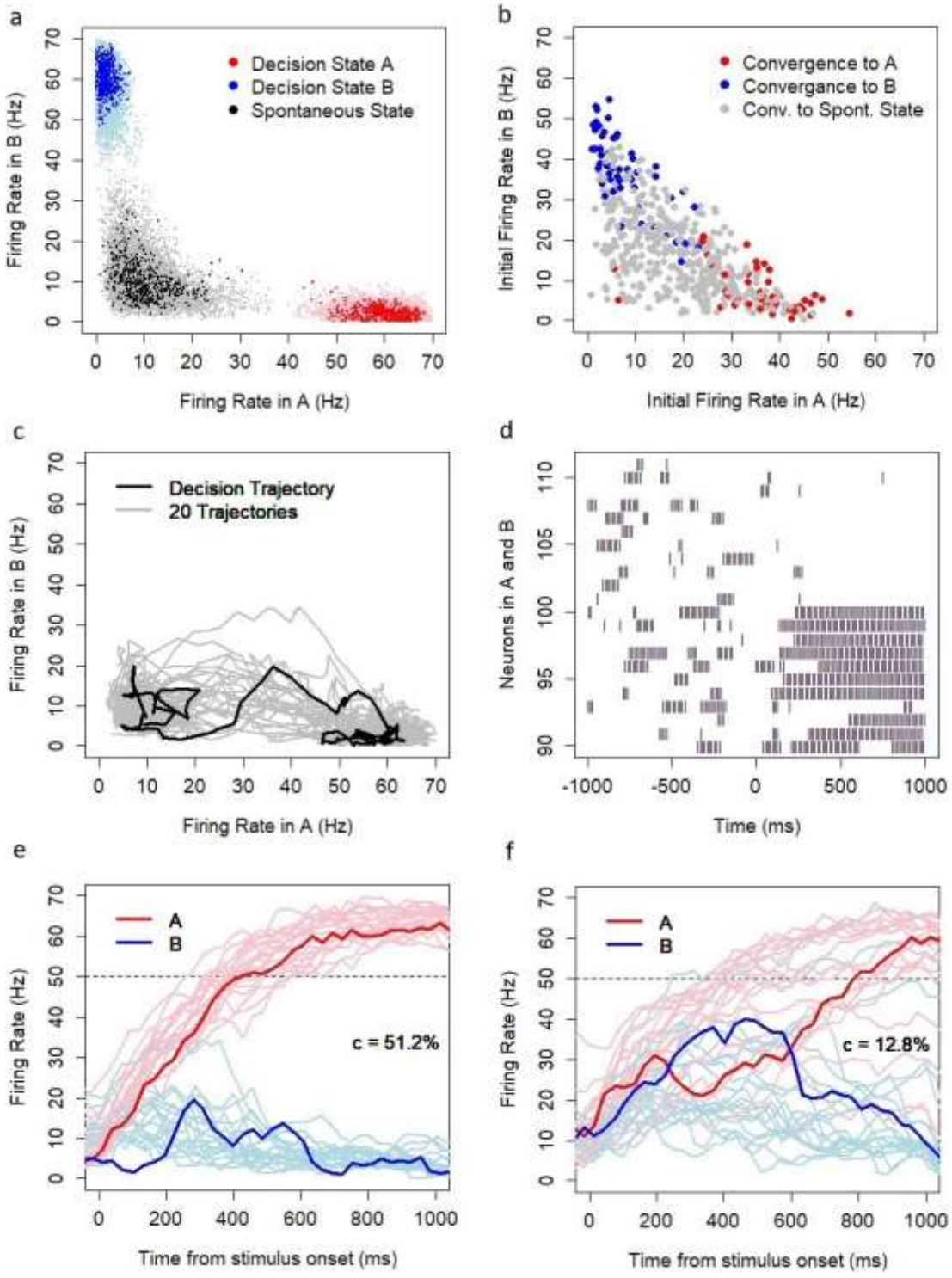

Figure 8: a. Attractor states: spontaneous state (black), decision states A (red) and B (blue), regular color N=1500 data points, light hue N=30000 data points. b. Basins of attraction: convergence to a steady-state within 1000s from randomly defined initial state measured within 50ms after network initialization. c. Decision Trajectories for model runs with coherence level c = 51.2%. d. Spiking activity of neurons in pools A (#90-100) and B (#101-111) before stimulus onset (-1000ms to 0) and after providing input to pool A only (0 to 1000ms). e. Firing rate in pools A and B for model runs with coherence level c = 51.2%. f. Firing rate in pools A and B for model runs with coherence level c = 12.8%.

Emergent system dynamics are consistent with neurophysiologic observations. The model has three attractor states (Fig. 8a): the spontaneous state with a low firing rate 4-20Hz (mean firing rate in the decision pool: 10.3Hz, SD = 5.2), and two decision states when the vast majority of neurons in the winning decision set (either A or B) fire with a high firing rate 51-66Hz (mean: 59.7Hz, SD = 4.7). When the model is in one of the decision states, the firing rate in the dominated pool is suppressed 0-5Hz (mean: 2Hz, SD = 1.4). With no inputs, all three steady states are semi-stable in the sense that the model maintains each state for a period of time, but the chance of escaping from the state is non-zero, and the system eventually moves to another state. The estimated median time to escape from the spontaneous state is in the range of 35s, and the escape dynamics follow exponential decay (estimated relaxation time: 50s). The estimated median time to escape from the decision state is in the range of 10s. Interestingly, the process does not follow exponential decay. The leak rate is not constant and diminishes over time. The semi-stability of the decision states ensures the ability of the model to serve as the working memory system. The boundaries of basins of attraction are fuzzy (Fig. 8b); a similar randomly chosen initial state can converge to a different steady state. This effect signifies that the model behaves chaotically.

When inputs are provided, the system moves from the spontaneous state to one of the decision states (Fig. 8c). Spiking activity of neurons is consistent with the neurophysiologic observations: in the spontaneous state, neurons fire irregularly and generate bursting activities (Fig. 8d, time: -1000 to 0ms). When an input is provided to one of the decision sets, the neurons in this set switch from low firing rate to high firing rate while neurons in the opposite set are silenced (Fig. 8d, time: 0 to 1000ms). The system facilitates probabilistic decision-making. The probability of reaching the decision state increases with the stimulus strength and stimulus duration while the time to reach the decision state decreases. The ramping activity of neurons and the speed of neuronal integration depend on the relative strength of inputs to both decision sets. In an easy task with a higher difference between inputs (Fig. 8e, coherence c = 51.2%), the system converges to the correct decision in most cases, and the reaction time is short. In a difficult task with a lower difference between inputs (Fig. 8f, coherence c =

12.8%), the system often converges to erroneous decisions and the reaction time on correct decisions is longer. For simplicity of notation, I denote by A and B both the decision sets, i.e., pools of neurons in the system, and the decision states, i.e., states of the entire system when the pools A or B fire with high frequency.

Model predictions were validated based on the dot motion discrimination experiments (Shadlen and Newsome, 2001; Roitman and Shadlen, 2002). In these experiments, monkeys react to a display of dots moving coherently to one of two possible directions among a broader set of randomly moving dots. The task is to identify the direction and the difficulty of the task depends on the coherence level c, the percentage of dots (0 -100%) moving coherently to one of the directions. The experiments are conducted in two distinct decision paradigms: working-memory (fixed duration) paradigm when the subject is requested to provide a response after a fixed (usually randomized) time after stimulus expires or reaction-time paradigm when the subject provides a response after stimulus onset whenever ready. In these experiments, neurons in the LIP area display a ramping to threshold activity consistent with the monkey's behavioral response. Experimental data reveal the characteristic relationship between the coherence level and the decision accuracy (percentage of correct decisions), which follows the Weibull psychometric function:

$$\%\, correct = 1 - \frac{1}{2} * \exp(-\left(\frac{c}{\alpha}\right)^{\beta})$$

where c is the coherence level and α, β are parameters. The shape of the relationship is consistent between experiments and decision paradigms, while the estimated parameters α and β vary: α = 15, β = 1.1 in the Shadlen and Newsome experiment, and α = 6, β = 1.7 in the Roitman and Shadlen experiment (reported after Wang, 2002). Under the reaction-time decision paradigm, response time increases with task difficulty and is shorter for correct decisions and longer for erroneous decisions across all coherence levels (c > 0).

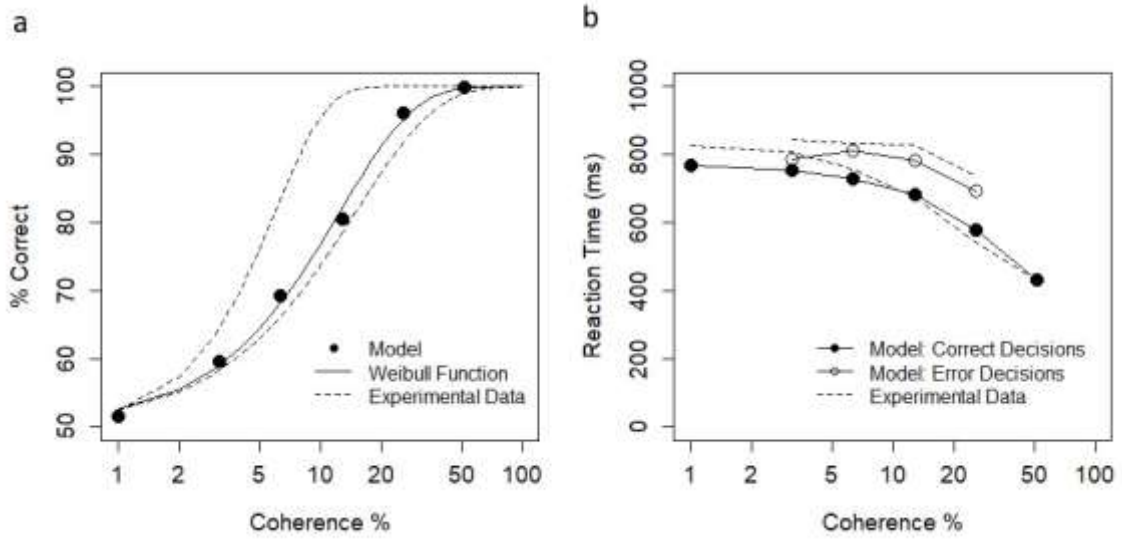

Figure 9: Model predictions for the dot motion discrimination task. a. Psychometric Function: N=12000 model runs (2000 per coherence level c = 0, 3.2%, 6.4%, 12.8%, 25.6% and 51.2%), SEM: 0.09 – 1.14; approximation with the Weibull function: $\alpha = 12.5$ and $\beta = 1.18$; experimental data (Shadlen and Newsome, 2001; Roitman and Shadlen, 2002). b. Reaction time (RT) as a function of correct and erroneous decisions and coherence level, SEM: 2.5 – 45.3; experimental data: the weighted average from two monkeys (Roitman and Shadlen, 2002).

Model predictions are consistent with the experimental data. Decision accuracy follows the psychometric function with realistic parameters $\alpha = 12.5$, $\beta = 1.18$ (Fig. 9a). Mean reaction times (RT) fit the observed patterns and produce realistic values (Fig. 9b). The absolute difference between estimated RT and the experimental data (the weighted average from two monkeys; Roitman and Shadlen, 2002) is in the range from <1 to 58ms (for correct decisions, coherence level 51.2% and erroneous decisions, coherence level 3.2%, respectively). The average discrepancy between model predictions and the experiment is 35ms (4.6%) across correct and erroneous decisions and various coherence levels.

Results are based on N= 12000 simulations (2000 per coherence level) using standard values of control parameters. Poisson inputs λ_A and λ_B (sampled each 30ms over the period of 2s after stimulus onset) were assumed to be linearly dependent on the coherence level c = 0, 3.2%, 6.4%, 12.8%, 25.6% and 51.2%:

$$\lambda_A = \lambda_0 \frac{1+c}{2}$$

$$\lambda_B = \lambda_0 \frac{1-c}{2}$$

where $\lambda_0 = 15$. The linear relationship between stimulus and inputs to the decision system is in-line with previous practice (Britten et al, 1993; Wang, 2002; Wong and Wang, 2006) and the observation that the firing rate of MT neurons (providing inputs to the sensory decision system in the LIP area) is the linear function of motion strength. Stimulus onset followed 1000ms of spontaneous model run. The decision threshold was set at the level of 52.5Hz. The firing rate was calculated based on 30ms lags sampled each 10ms. No decisions, decisions that took longer than 2000ms or were made earlier than 100ms after stimulus onset were removed (2.5%). No non-decision time was assumed.

The model exhibits a non-linear integration consistent with experiments (Peixoto et al., 2021). The sensitivity of the decision variable to changes in inputs decreases with the amount of integration and time from the stimulus onset (unpublished).

Code Availability: The model was implemented in R (R Core Team, 2021) version 4.1.1 (2021-08-10). Simulation code and databases generated with the code are publicly available: https://github.com/MarcinPenconek/Computational-Analysis-of-Speed-Accuracy-Tradeoff

Acknowledgements: The author would like to express his gratitude to Andrzej Wróbel and Daniel Wójcik for inspiration, discussions, and comments on the manuscript.

Additional Information: The author declares no competing interests.

References:

Bogacz, R., Brown, E., Moehlis, J., Holmes, P., & Cohen, J. D. (2006). The physics of optimal decision making: a formal analysis of models of performance in two-alternative forced-choice tasks. *Psychological Review*, *113*(4), 700-765.

Bogacz, R., Wagenmakers, E. J., Forstmann, B. U., & Nieuwenhuis, S. (2010). The neural basis of the speed–accuracy tradeoff. *Trends in Neurosciences*, *33*(1), 10-16.

Britten, K. H., Shadlen, M. N., Newsome, W. T., & Movshon, J. A. (1992). The analysis of visual motion: a comparison of neuronal and psychophysical performance. *Journal of Neuroscience*, *12*(12), 4745-4765.

Britten, K. H., Shadlen, M. N., Newsome, W. T., & Movshon, J. A. (1993). Responses of neurons in macaque MT to stochastic motion signals. *Visual neuroscience*, *10*(6), 1157-1169.

Chittka, L., Skorupski, P., & Raine, N. E. (2009). Speed–accuracy tradeoffs in animal decision making. *Trends in Ecology & Evolution*, *24*(7), 400-407.

Dayan, P., & Abbott, L. F. (2001). *Theoretical neuroscience: computational and mathematical modeling of neural systems*. Computational Neuroscience Series.

Doppelmayr, M., Klimesch, W., Stadler, W., Pöllhuber, D., & Heine, C. (2002). EEG alpha power and intelligence. *Intelligence*, *30*(3), 289-302.

Forstmann, B. U., Dutilh, G., Brown, S., Neumann, J., Von Cramon, D. Y., Ridderinkhof, K. R., & Wagenmakers, E. J. (2008). Striatum and pre-SMA facilitate decision-making under time pressure. *Proceedings of the National Academy of Sciences*, *105*(45), 17538-17542.

Furman, M., & Wang, X. J. (2008). Similarity effect and optimal control of multiple-choice decision making. *Neuron*, *60*(6), 1153-1168.

Garrett, H. E. (1922). *A study of the relation of accuracy to speed* (Vol. 8). Columbia University.

Gold, J. I., & Shadlen, M. N. (2002). Banburismus and the brain: decoding the relationship between sensory stimuli, decisions, and reward. *Neuron*, *36*(2), 299-308.

Goldman, R. I., Stern, J. M., Engel Jr, J., & Cohen, M. S. (2002). Simultaneous EEG and fMRI of the alpha rhythm. *Neuroreport*, *13*(18), 2487–2492.

Haegens, S., Nácher, V., Luna, R., Romo, R., & Jensen, O. (2011). α-Oscillations in the monkey sensorimotor network influence discrimination performance by rhythmical inhibition of neuronal spiking. *Proceedings of the National Academy of Sciences*, *108*(48), 19377-19382.

Hanks, T., Kiani, R., & Shadlen, M. N. (2014). A neural mechanism of speed-accuracy tradeoff in macaque area LIP. *Elife*, *3*, e02260.

Hebb, D. O. (2005). *The organization of behavior: A neuropsychological theory*. New York, NY: John Wiley & Sons.

Heitz, R. P. (2014). The speed-accuracy tradeoff: history, physiology, methodology, and behavior. *Frontiers in Neuroscience*, *8*, 150.

Heitz, R. P., & Schall, J. D. (2012). Neural mechanisms of speed-accuracy tradeoff. *Neuron*, *76*(3), 616-628.

Ivanoff, J., Branning, P., & Marois, R. (2008). fMRI evidence for a dual process account of the speed-accuracy tradeoff in decision-making. *PLoS one*, *3*(7), e2635.

Kable, J. W., & Glimcher, P. W. (2009). The neurobiology of decision: consensus and controversy. *Neuron*, *63*(6), 733-745.

Klimesch, W., Sauseng, P., & Hanslmayr, S. (2007). EEG alpha oscillations: the inhibition–timing hypothesis. *Brain research reviews*, *53*(1), 63-88.

Klimesch, W., Vogt, F., & Doppelmayr, M. (1999). Interindividual differences in alpha and theta power reflect memory performance. *Intelligence*, *27*(4), 347-362.

Kuc, A. K., Kurkin, S. A., Maksimenko, V. A., Pisarchik, A. N., & Hramov, A. E. (2021). Monitoring Brain State and Behavioral Performance during Repetitive Visual Stimulation. *Applied Sciences*, *11*(23), 11544.

Laufs, H., Kleinschmidt, A., Beyerle, A., Eger, E., Salek-Haddadi, A., Preibisch, C., & Krakow, K. (2003a). EEG-correlated fMRI of human alpha activity. *Neuroimage*, *19*(4), 1463-1476.

Laufs, H., Krakow, K., Sterzer, P., Eger, E., Beyerle, A., Salek-Haddadi, A., & Kleinschmidt, A. (2003b). Electroencephalographic signatures of attentional and cognitive default modes in spontaneous brain activity fluctuations at rest. *Proceedings of the national academy of sciences*, *100*(19), 11053-11058.

Lo, C. C., & Wang, X. J. (2006). Cortico–basal ganglia circuit mechanism for a decision threshold in reaction time tasks. *Nature Neuroscience*, *9*(7), 956-963.

Lo, C. C., Wang, C. T., & Wang, X. J. (2015). Speed-accuracy tradeoff by a control signal with balanced excitation and inhibition. *Journal of Neurophysiology*, *114*(1), 650-661.

Luce, R.D. (1986). *Response times*. New York, NY: Oxford University Press.

Moosmann, M., Ritter, P., Krastel, I., Brink, A., Thees, S., Blankenburg, F., Taskin, B., Obrig, H., & Villringer, A. (2003). Correlates of alpha rhythm in functional magnetic resonance imaging and near infrared spectroscopy. *Neuroimage*, *20*(1), 145-158.

Newsome, W. T., Britten, K. H., & Movshon, J. A. (1989). Neuronal correlates of a perceptual decision. *Nature*, *341*(6237), 52-54.

Paluch, K., Jurewicz, K., & Wróbel, A. (2021). Beyond Difference in Reaction Time: Understanding Neuronal Activity during the Preparatory Period of the Decision Process. *Journal of Cognitive Neuroscience*, *33*(2), 263-278.

Peixoto, D., Verhein, J. R., Kiani, R., Kao, J. C., Nuyujukian, P., Chandrasekaran, C., Brown, J., Fong, S., Ryu, S. I., Shenoy, K. V., & Newsome, W. T. (2021). Decoding and perturbing decision states in real time. *Nature*, *591*(7851), 604-609.

Penconek, M. (2020). Decision making model based on attractor network with binary neurons. *Procedia Computer Science*, *176*, 1930-1939.

R Core Team (2021). R: A language and environment for statistical computing. R Foundation for Statistical Computing, Vienna, Austria. URL https://www.R-project.org/.

Rafiei, F., & Rahnev, D. (2021). Qualitative speed-accuracy tradeoff effects that cannot be explained by the diffusion model under the selective influence assumption. *Scientific Reports*, *11*(1), 1-19.

Ratcliff, R. (1978). A theory of memory retrieval. *Psychological Review*, *85*(2), 59-108.

Ratcliff, R., & Kang, I. (2021). Qualitative speed-accuracy tradeoff effects can be explained by a diffusion/fast-guess mixture model. Scientific Reports, 11(1), 1-9.

Roitman, J. D., & Shadlen, M. N. (2002). Response of neurons in the lateral intraparietal area during a combined visual discrimination reaction time task. *Journal of Neuroscience*, *22*(21), 9475-9489.

Schall, J. D. (2001). Neural basis of deciding, choosing and acting. *Nature Reviews Neuroscience*, *2*(1), 33-42.

Shadlen, M. N., & Newsome, W. T. (2001). Neural basis of a perceptual decision in the parietal cortex (area LIP) of the rhesus monkey. *Journal of Neurophysiology*, *86*(4), 1916-1936.

Smith, P. L., & Ratcliff, R. (2004). Psychology and neurobiology of simple decisions. *Trends in Neurosciences*, *27*(3), 161-168.

Rolls, E. T. (2014). *Emotion and decision-making explained*. Oxford University Press.

Sadato, N., Nakamura, S., Oohashi, T., Nishina, E., Fuwamoto, Y., Waki, A., & Yonekura, Y. (1998). Neural networks for generation and suppression of alpha rhythm: a PET study. *Neuroreport*, *9*(5), 893-897.

Standage, D., Blohm, G., & Dorris, M. C. (2014). On the neural implementation of the speed-accuracy tradeoff. *Frontiers in Neuroscience*, *8*, 236.

Standage, D., You, H., Wang, D., & Dorris, M. C. (2011). Gain modulation by an urgency signal controls the speed–accuracy tradeoff in a network model of a cortical decision circuit. *Frontiers in Computational Neuroscience*, *5*, 7.

Standage, D., You, H., Wang, D. H., & Dorris, M. C. (2013). Trading speed and accuracy by coding time: a coupled-circuit cortical model. *PLoS Computational Biology*, *9*(4), e1003021.

Van Veen, V., Krug, M. K., & Carter, C. S. (2008). The neural and computational basis of controlled speed-accuracy tradeoff during task performance. *Journal of Cognitive Neuroscience*, *20*(11), 1952-1965.

Vogt, F., Klimesch, W., & Doppelmayr, M. (1998). High-frequency components in the alpha band and memory performance. *Journal of Clinical Neurophysiology*, *15*(2), 167-172.

Wang, X. J. (2002). Probabilistic decision making by slow reverberation in cortical circuits. *Neuron*, *36*(5), 955-968.

Wickelgren, W. A. (1977). Speed-accuracy tradeoff and information processing dynamics. *Acta Psychologica*, *41*(1), 67-85.

Wong, K. F., & Wang, X. J. (2006). A recurrent network mechanism of time integration in perceptual decisions. *Journal of Neuroscience*, *26*(4), 1314-1328.

Woodworth, R. S. (1899). Accuracy of voluntary movement. *The Psychological Review: Monograph Supplements*, *3*(3), i.

Wójcik, D. K. (2018). The Kinematics of Spike Trains. *Acta Physica Polonica B*, *49*(12), 2127-2138.